Int. J. Appl. Ceram. Technol., 4 [6] 564–570 (2007)

International Journal of Applied Ceramic Technology
Ceramic Product Development and Commercialization

Microstructural Development of ZnO Pellets Doped with Different Vanadium Oxides (V_2O_5 and V_2O_3)

Francisco Méndez-Martínez, Miriam J. Venegas, and Heriberto Pfeiffer*

Departamento de Materiales Metálicos y Cerámicos, Instituto de Investigaciones en Materiales, Universidad Nacional Autónoma de México, México D.F., Mexico

This work presents the effect of zinc oxide (ZnO) ceramics, doped with different percentages of vanadium trioxide (V_2O_3) and vanadium pentoxide (V_2O_5). Samples were analyzed by X-ray diffraction and scanning electron microscopy. The addition of V_2O_3 or V_2O_5 produced changes in the composition and morphology of the pellets. In both cases, different zinc vanadates were detected as secondary phases: α-$Zn_3(VO_4)_2$ and $Zn_4V_2O_9$. Furthermore, when the vanadium concentration was equal to or higher than 3 wt%, the presence of filaments was detected on the surface of the pellets. These filaments were produced due to vanadium segregation. However, this effect was only observed at the surface of the pellets. On the bulk, the filaments were not observed. Instead, vanadium was found at the interfaces between the ZnO grains and at triple points, as it could be expected.

Introduction

Zinc oxide (ZnO)-based materials have been widely studied for different kinds of applications, such as gas sensors, piezoelectric transducers, optical waveguides, electrodes, and varistors, among other applications.[1–5]

In general, all these applications depend on their structural properties, where the ceramic behavior is highly controlled by microstructural and surface features, such as composition, particle size, surface area, and porosity. Nevertheless, in some cases when consolidated samples are doped, the dopants tend to diffuse around the particles and segregate at the surface and/or at triple points into the bulk of the pellets. Consequently, secondary phases are produced, which in most of the cases modified the properties of the material.[6] For example, in the ZnO varistors all these features are very important, as electrical properties depend on the interfaces among the particles and the surface of the pellets.[1,7–15]

Although ZnO doped with small quantities of vanadium pentoxide, alone or mixed with other metal oxides has been reported, there is no research on the addition of vanadium trioxide (V_2O_3) in the same kind of systems.[10,11,16] This vanadium oxide has a different reactivity due to the vanadium oxidation state. Then, the chemical reactivity of this oxide with ZnO may vary, in comparison with vanadium pentoxide (V_2O_5). Furthermore, papers in the literature report the addition of <1 mol% of V_2O_5. Then, the aim of this work was to analyze and compare the microstructure evolution of ZnO pellets produced by the addition of two different

This work was financially supported by the project 46522-Q SEP-CONACYT, Mexico.
*pfeiffer@iim.unam.mx

vanadium oxides, V_2O_5 and V_2O_3, in higher proportions than those reported typically. It has been performed in order to investigate whether there is any difference when ZnO is doped with two different vanadium oxides, where vanadium possesses different oxidation states, and therefore different reactivity.

Experimental Procedure

ZnO pellets were synthesized using high-purity powders of ZnO (99.9%, Aldrich, St. Louis, MO), V_2O_5 (98+%, Aldrich), and V_2O_3 (99%, Aldrich). Powders of ZnO and V_2O_5 or V_2O_3 were mixed for 3 h in deionized water, using a magnetic stirrer. The samples were dried at 70°C, and pressed into 10-mm-diameter pellets. Latter pellets were heat treated for 4 h at different temperatures: 300°C, 500°C, 700°C, 800°C, 900°C, 1000°C, and 1100°C. After the sintering process, the samples were air cooled to room temperature. The final density obtained of the pellets was equal to 85–90% of the theoretical density. The pellets were prepared using different molar percentages of the vanadium oxides. V_2O_5 or V_2O_3 were added at levels of 0.5, 1.0, 3.0, and 5.0 mol%.

All the pellets heat treated at different temperatures were characterized by X-ray diffraction (XRD) and scanning electron microscopy (SEM). To obtain the XRD patterns, a slower detailed scan was necessary to enable the various secondary phases to be identified. A diffractometer (D8 Advance, Bruker AXS, Madison, WI) coupled to a copper anode X-ray tube was used. The different compounds were identified by their corresponding Joint Committee on Powder Diffraction Standards (JCPDS) files, and the relative percentages, of each phase, were estimated from the total area under the most intense diffraction peaks. The estimated experimental error was $\pm 3\%$. A scanning electron microscope (Stereoscan 440 Leica/Cambridge, St. Gallen, Switzerland) was used to determine the particle size, morphology, and composition of the materials. All these features were observed in secondary electron image, backscattered electron image (BSEI), and elemental analysis (EDS).

In order to analyze whether the pellets have the same chemical composition and morphology on the surface and the bulk, a set of samples was ground down ($\approx$ 2–3 mm) and etched, using a sulfuric acid solution (1 N) for 5 h. The pellets were, then, washed in deionized water several times to eliminate excess sulfuric acid. This chemical treatment was performed in order to analyze the microstructure of the core of the pellets.

Results

All the samples examined by XRD were mainly composed by ZnO, and only small quantities of secondary phases were detected. Figure 1 presents the XRD patterns of the ZnO doped with different quantities of V_2O_3 and V_2O_5. First, when the samples were doped

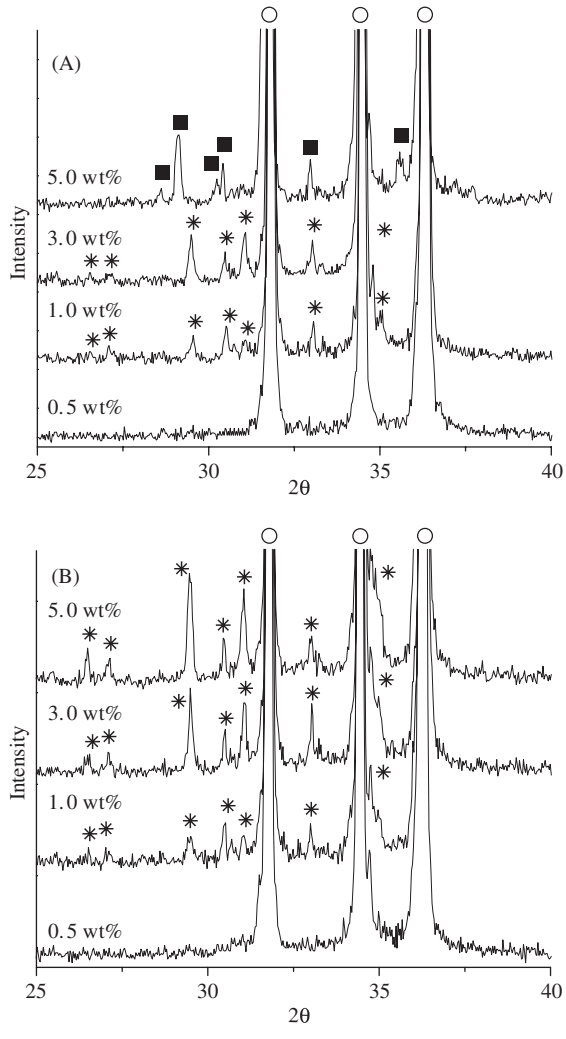

Fig. 1. X-ray diffraction patterns of the samples containing different quantities of (A) V_2O_5 or (B) V_2O_3. The three main peaks correspond to the ZnO phase and each of the secondary phases is labeled as ○, ZnO; ∗, α-$Zn_3(V_2O_4)_2$; and ■, $Zn_4V_2O_9$.

with 0.5 wt%, of V_2O_3 or V_2O_5, the XRD patterns did not indicate the presence of different phases other than ZnO. Conversely, a zinc vanadate was found as a secondary phase when ZnO was doped with 1 and 3 wt% of any of the vanadium oxides. In both cases, the secondary phase detected was α-$Zn_3(VO_4)_2$, which has an orthorhombic crystalline structure (JCPDS file 34-0378).[17,18]

Finally, samples containing 5 wt% of V_2O_3 or V_2O_5 presented different behaviors. In the V_2O_3 case, the final composition was similar to those results obtained at lower vanadium concentrations, where ZnO and α-$Zn_3(VO_4)_2$ were the two phases detected. On the other hand, the sample doped with 5 wt% of V_2O_5 produced a different secondary phase, $Zn_4V_2O_9$ (JCPDS file 77-1757). However, when this pellet was ground down, $Zn_4V_2O_9$ disappeared, and the phases detected were ZnO and α-$Zn_3(VO_4)_2$ again.

In order to analyze the effect of the temperature on the formation of these secondary phases, a different set of samples, with 5 wt% of V_2O_3 or V_2O_5, was heat treated at different temperatures (Fig. 2). At low temperatures, between 300°C and 800°C, the only secondary phase detected by XRD was α-$Zn_3(VO_4)_2$. These results showed the formation of secondary phases even at very low temperatures (300°C) and the similarity of the samples. These results are in good agreement with the ZnO–V_2O_5 phase diagram, which did not show any solid solubility of vanadium oxide in ZnO.[19,20] However, when the temperature was increased to 900°C or more, α-$Zn_3(VO_4)_2$ disappeared and $Zn_4V_2O_9$ was produced.

The surface morphology of the pellets was determined by SEM. SEM analyses were performed on all the pellets, and the results were very similar between samples doped with V_2O_5 and V_2O_3. Thus, only the results obtained for ZnO doped with V_2O_3 are presented. The surface of the ZnO pellet, doped with 0.5 wt% of V_2O_3, presented particles with different sizes (Fig. 3A). The largest particles showed a diameter of 15–20 μm, while the smallest were about 2 μm in size, where their abundance was estimated to be 32% and 68%, respectively. Furthermore, the porosity of the samples did not seem to be high.

When the pellets were doped with 1 and 3 wt% of V_2O_3, the morphology of the surfaces changed. First, the particle size tended to be more homogeneous (Fig. 3B). Although the large particles remained there, the small particles had a tendency to disappear or to grow. In these cases, the different particle sizes were 15–20 and 4–5 μm, in average, with abundances of 67% and 33%, respectively. As in the first composition, the porosity did not seem to change. Moreover, a different effect became evident: the formation of some filament structures, growing over the surface of the pellets. These filaments were not considered in the abundance calculation. However, the presence of filaments was dramatically evidenced when the quantity of V_2O_3 increased to 5 wt% (Fig. 3C). In this sample, the particle

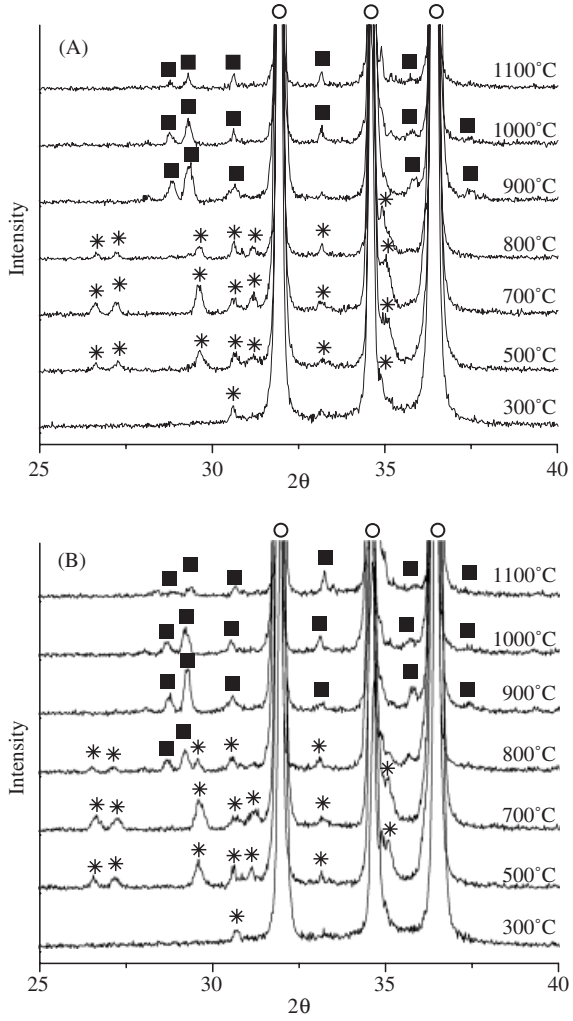

Fig. 2. X-ray diffraction patterns of the samples containing 5 wt% of (A) V_2O_5 or (B) V_2O_3, heat treated at different temperatures. The three main peaks correspond to the ZnO phase and each of the secondary phases is labeled as ○, ZnO; ∗, α-$Zn_3(V_2O_4)_2$; and ■, $Zn_4V_2O_9$.

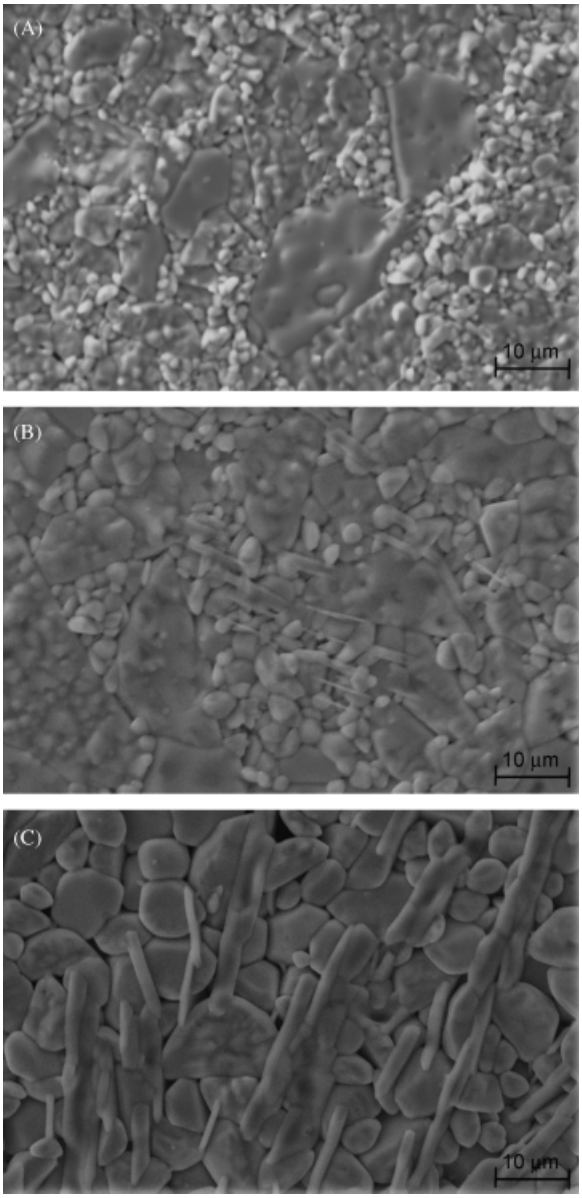

Fig. 3. Scanning electron microscopic images of samples containing 0.5 wt% of V_2O_3 (A), 3.0 wt% of V_2O_3 (B), and 5.0 wt% of V_2O_3 (C).

size was completely homogeneous, being equal to 5–10 µm. Therefore, as the initial ZnO particle size was around 1–2 µm, according to Aldrich, the particle size of ZnO is enhanced and homogeneously controlled by the addition of vanadium oxides.

A closer examination of the ZnO pellet doped with 5 wt% of V_2O_3 showed that filaments were growing all around the surface of the pellets. Furthermore, the BSEI strongly suggests that the filaments have a different composition, due to the contrast differences observed (Fig. 4). In addition, elemental analyses (EDS) were performed, over the different parts of the pellet. First, a general EDS analysis, of the surface of the pellet, gave the following results: oxygen 56.01 at.%, zinc 41.31 at.%, and vanadium 2.68 at.%. These results are in excellent agreement with the nominal composition of O = 50.66 at.%, Zn = 46.68 at.%, and V = 2.65 at.%, which corresponds to the ZnO doped with 5 wt% of V_2O_3. Nevertheless, specific EDS analyses over the two kinds of particles (filaments and polygonal particles) produced very different results. While the polygonal particles did not contain vanadium, the filaments presented a very high level of vanadium (13.78 at.%), as can be seen in Table I.

Finally, a further analysis was performed. In this case, the samples containing 5 wt% of vanadium oxides

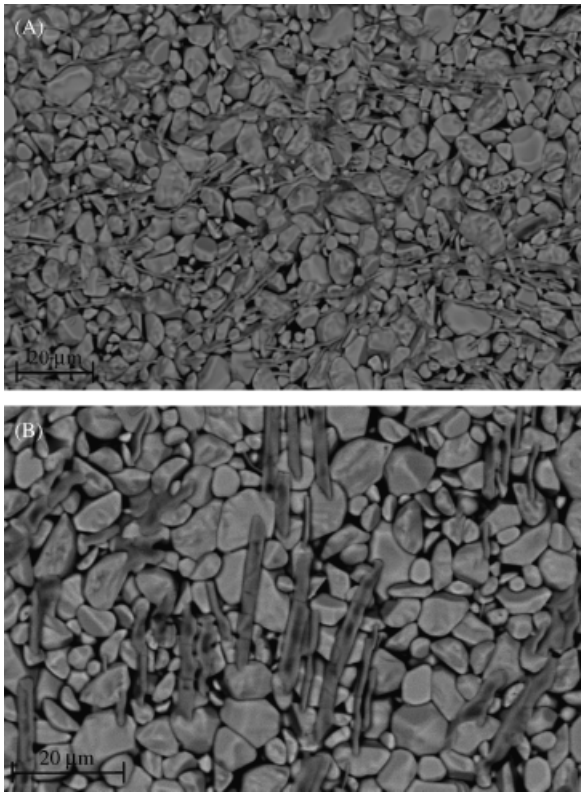

Fig. 4. Backscattered micrographs of the sample containing 5.0 wt% of V_2O_3. The dark regions have a lower mean atomic number than the average and are vanadium-rich phases.

Table I. Superficial EDS Analyses of the Different Sections of the ZnO Pellet Doped with 5 wt% of V_2O_3

	Type of particle		
Element	Polygonal (at.%)	Filament (at.%)	Theoretical composition of $Zn_3(VO_4)_2$ (at.%)
Zn	44.47	27.34	23.07
V	—	13.78	15.38
O	55.53	58.88	61.53

were ground down and etched on sulfuric acid as described in the experimental section. First, the XRD pattern of the ZnO pellet doped with 5 wt% of V_2O_3 gave results similar to those obtained over the surface of the pellet. The main phase corresponds to ZnO, and α-$Zn_3(VO_4)_2$ was detected as a secondary phase. On the other hand, the composition of the sample doped with 5 wt% of V_2O_5, changed. $Zn_4V_2O_9$ was not found; instead, α-$Zn_3(VO_4)_2$ was obtained as a secondary phase.

In addition, SEM analyses of these two pellets did not show the presence of filaments or any kind of particles containing a high level of vanadium (Fig. 5). The particle size, of the ZnO grains into the bulk of the pellet, was similar to the particle size determined at the surface, 5–10 μm. EDS analyses indicated that vanadium is mainly deposited at the border of the particles or at triple points, as it could be expected. These results

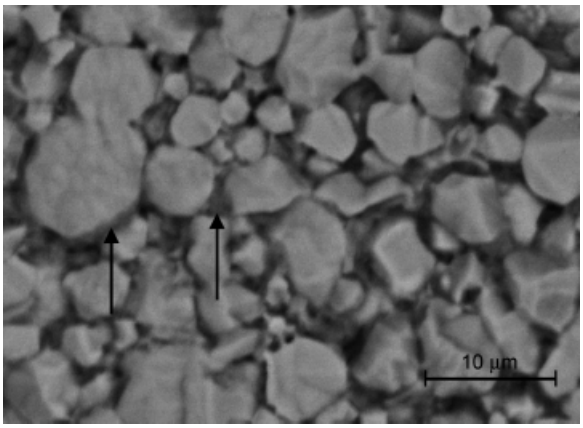

Fig. 5. Backscattered image of the center of the pellet containing 5.0 wt% of V_2O_3. The arrows illustrate the vanadium-rich regions, grain borders, or triple points.

Table II. Bulk EDS Analyses of the Different Sections of the ZnO Pellet Doped with 5 wt% of V_2O_3

	Area	
Element	Polygonal (at.%)	Frontier and triple points (at.%)
Zn	48.21	28.76
V	—	6.46
O	51.79	64.78

are summarized in Table II. Moreover, the vanadium content decreased to 1.33 at.%, in comparison with the vanadium detected at the surface of the pellet (2.68 at.%).

In sum, SEM and EDS analyses showed that samples changed their morphology as a function of the vanadium content. In addition, vanadium was not distributed uniformly throughout the surface of the samples; it segregated, producing filaments.

Discussion

To summarize, from XRD two different secondary phases were identified: α-$Zn_3(VO_4)_2$ and $Zn_4V_2O_9$. These measurements are in agreement with the SEM results, where morphological information and mainly the BSEI evidenced the presence of two phases at least.

Two different secondary phases, α-$Zn_3(VO_4)_2$ and $Zn_4V_2O_9$, were determined on these samples using V_2O_3 and V_2O_5. In both cases, the $Zn_4V_2O_9$ was produced when the temperature reached 900°C or at higher temperatures. In a previous paper,[10] it was proposed that $Zn_4V_2O_9$ is always produced in the presence of α-$Zn_3(VO_4)_2$, and the $Zn_4V_2O_9$ formation rate seems to be slower than that of α-$Zn_3(VO_4)_2$. Moreover, according to the ZnO–V_2O_5 phase diagram,[19,20] a liquid phase is produced at 890 ± 10°C. This temperature fit very well with the $Zn_4V_2O_9$ formation. Therefore, the results obtained in this work may be explained in terms of reactivity. Apparently, $Zn_4V_2O_9$ is produced at the surface of the pellets through a previous α-$Zn_3(VO_4)_2$ formation, which fuses and then reacts with ZnO (reaction 1).

$$\alpha\text{-}Zn_3(VO_4)_2 + ZnO \rightarrow Zn_4V_2O_9 \qquad (1)$$

Furthermore, although the relative proportions of the secondary phases were unambiguous, it seems that

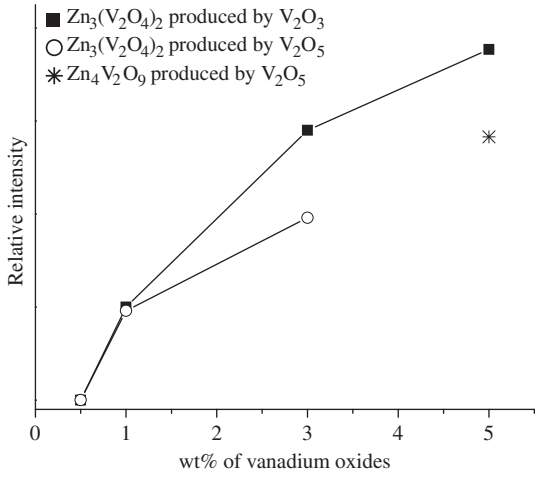

Fig. 6. Plot of the relative proportions of secondary phases, as a function of the vanadium oxide percentages.

the quantity of each phase increases as a function of the vanadium, as expected (Fig. 6). However, according to the results, it is clear that the formation of α-$Zn_3(VO_4)_2$ is produced at temperatures lower than 800°C and, once it has been produced it converts into $Zn_4V_2O_9$ at 900°C or higher temperatures.

In the V_2O_3 samples, the α-$Zn_3(VO_4)_2$ formation detected by XRD indicates vanadium oxidation from V^{3+} to V^{5+}, as it could be expected, with the consequent addition of oxygen (reaction (2)). On the other hand, α-$Zn_3(VO_4)_2$ and $Zn_4V_2O_9$ formation, using V_2O_5, did not require any oxidation process (reaction (3)).

$$3\ ZnO + V_2O_3 + O_2 \rightarrow \alpha\text{-}Zn_3(VO_4)_2 \qquad (2)$$

$$3\ ZnO + V_2O_5 \rightarrow \alpha\text{-}Zn_3(VO_4)_2 \qquad (3)$$

It is evident that vanadium oxidation, from V_2O_3 to V_2O_5, occurs at lower temperatures than 500°C, but if the V_2O_3 oxidation depends on the presence of oxygen, reaction (2) must be limited to the surface of the pellet or at least the kinetic of the reaction may be diminished into the bulk of the pellets. In order to study this hypothesis, the pellets were ground down and etched to analyze the chemical composition at the bulk of the pellet. Nevertheless, XRD results showed the presence of the same secondary phase α-$Zn_3(VO_4)_2$ (data not showed). Therefore, there must be some availability of oxygen atoms, which allows the formation of α-$Zn_3(VO_4)_2$ even in the bulk of the pellets. In fact, ZnO produces nonstoichiometric phases under an oxidizing or a reducing atmosphere.[21,22] A typical example is the production of $Zn_{1+x}O$ in reducing atmospheres. Then, the "excess" of oxygen produced, by the reducing atmosphere of this reaction, must produce α-$Zn_3(VO_4)_2$ even in the bulk of the pellets.

SEM analyses are in excellent agreement with the XRD results. The backscattered electron micrographs and the chemical composition strongly suggest that the filaments were not composed by ZnO, which may be produced due to the α-$Zn_3(VO_4)_2$ fusion and latter solidification as $Zn_4V_2O_9$. Actually, the differences in contrast seen in Fig. 4B arose from the differences in the mean atomic number, $\bar{Z}$, of ZnO ($\bar{Z} = 19$) and a secondary phase, perhaps the secondary phase detected by XRD, α-$Zn_3(VO_4)_2$ ($\bar{Z} = 15.38$). Therefore, the backscattered electron coefficient, η, has to present differences between the two phases, through the following equation:[23]

$$\eta = 0.0254 + 0.016\bar{Z} - 1.86 \times 10^{-4}\bar{Z}^2 + 8.3 \times 10^{-7}\bar{Z}^3 \qquad (4)$$

Hence, η decreases from 0.217 for ZnO, the lighter phase in Fig. 4B, to 0.179 for $Zn_3(VO_4)_2$, the darker phase. This hypothesis was confirmed by the EDS study. EDS analyses of the polygonal particles showed that this sort of particles practically do not contain vanadium (Table I). All the vanadium was detected on the filaments. Additionally, EDS analyses in the bulk of the pellets showed a deficiency of vanadium in comparison with the quantity of vanadium detected at the surface.

For these reasons, the results strongly suggest that vanadium diffuses and segregates, from the bulk to the surface of the pellets, producing filaments of zinc vanadates. This idea was supported by the ZnO–V_2O_5 phase diagram, which describes the fusion of secondary phases at $T \geq 900$°C. Specifically, α-$Zn_3(VO_4)_2$ is the first phase produced, according to the atomic percentages determined by EDS and by the XRD results. Later, $Zn_4V_2O_9$ is produced at the surface of the pellets.

Finally, although the solubility of V_2O_3 and V_2O_5 in ZnO was estimated to be ≤ 0.5 wt%, higher additions of vanadium oxides allowed controlling the particle size of the ZnO grains. Hence, as several physicochemical processes depend on grain–grain interfaces, the particle size is determinant. Therefore, the addition of vanadium oxides in ZnO helps to homogenize and

enhance the growth of the grains and could be considered as grain growth enhancers.

Conclusions

ZnO varistor ceramics have been prepared using ZnO with 0.5, 1.0, 3.0, and 5.0 wt% of V_2O_5 and V2O3. XRD analyses strongly suggest that α-$Zn_3(VO_4)_2$ formation is favored over the surface of the pellets at temperatures $\leq 800^{\circ}C$. On the contrary, $Zn_4V_2O_9$ was found in samples heat treated at higher temperatures ($\geq 900^{\circ}C$). The synthesis of $Zn_4V_2O_9$ may be produced by the reaction of α-$Zn_3(VO_4)_2$ with ZnO.

A vanadium segregation effect was detected by SEM, for the samples containing 3 wt%, or more, of any of the vanadium oxides. First, the surface of the pellets showed the formation of filaments. In addition, BSEI and EDS analyses showed that these filaments are enriched in vanadium, having an elemental composition very close to the theoretical compositions of α-$Zn_3(VO_4)_2$. On the contrary, the ZnO grains practically did not contain vanadium. The latter results confirmed the vanadium segregation in the form of filaments over the surface of the pellets. Further analyses performed in the bulk of the pellets suggested that the filaments are just produced on the surface.

No significant difference was found when the samples were doped with V_2O_3 or V_2O_5. In V_2O_3, vanadium is oxidized from +3 to +5, producing two different zinc vanadates α-$Zn_3(VO_4)_2$ or $Zn_4V_2O_9$, as the samples doped with V_2O_5, and no other change in the structure or composition of the pellets was observed.

Acknowledgments

The authors thank L. Baños and J. Guzman for technical help.

References

1. D. R. Clarke, "Varistor Ceramics," *J. Am. Ceram. Soc.*, 82 485–502 (1999).
2. J. Han, P. Q. Mantas, and A. M. R. Senos, "Defect Chemistry and Electrical Characteristics of Undoped and Mn-Doped ZnO," *J. Eur. Ceram. Soc.*, 22 49–59 (2002).
3. M. E. V. Costa, P. Q. Mantas, and J. L. Baptista, "Effect of Electrode Alterations on the AC Behaviour of Li_2O–ZnO Humidity Sensors," *Sensors Actuators B*, 27 312–314 (1995).
4. D. J. Nagaraju and S. B. Krupanidhi, "Temperature Dependent Transport Properties of $CuInSe_2$–ZnO Heterostructure Solar Cell," *J. Phys. Chem. Solids*, 67 1636–1642 (2006).
5. S. Dutta, H. E. Jackson, J. T. Boyd, F. S. Hickernell, and R. L. Davis, "Scattering Loss Reduction in ZnO Optical Waveguides by Laser Annealing," *Appl. Phys. Lett.*, 39 206–208 (1981).
6. R. Magri and A. Zunger, "Effects of Interfacial Atomic Segregation on Optical Properties of InAs/GaSb Superlattices," *Phys. Rev. B*, 64 1–5 (2001).
7. C. M. Wang, J. F. Wang, H. C. Chen, W. B. Su, G. Z. Zang, P. Qi, and M. L. Zhao, "Effects of CuO on the Grain Size and Electrical Properties of SnO_2-Based Varistors," *Mater. Sci. Eng. B*, 116 54–58 (2005).
8. B. S. Chiou and M. C. Chung, "Effect of Copper Additive on the Microstructure and Electrical Properties of Polycrystalline Zinc Oxide," *J. Am. Ceram. Soc.*, 75 3363–3368 (1992).
9. F. Apaydin, H. Özkan-Toplan, and K. Yildiz, "The Effect of CuO on the Grain Growth of ZnO," *J. Mater. Sci.*, 40 677–682 (2005).
10. H. Pfeiffer and K. M. Knowles, "Effects of Vanadium and Manganese Concentrations on the Composition, Structure and Electrical Properties of ZnO-rich MnO_2–V_2O_5–ZnO Varistors," *J. Eur. Ceram. Soc.*, 24 1199–1203 (2004).
11. H. H. Hng and K. M. Knowles, "Microstructure and Current–Voltage Characteristics of Multicomponent Vanadium-Doped Zinc Oxide Varistors," *J. Am. Ceram. Soc.*, 83 2455–2462 (2000).
12. C. T. Kuo, C. S. Chen, and I. N. Lin, "Microstructure and Nonlinear Properties of Microwave-Sintered ZnO–V_2O_5 Varistors: II, Effect of Mn_3O_4 Doping," *J. Am. Ceram. Soc.*, 81 2949–2956 (1998).
13. J. Han, A. M. R. Senos, and P. Q. Mantas, "Deep Donors in Polycrystalline Mn-Doped ZnO," *Mater. Chem. Phys.*, 75 117–120 (2002).
14. T. R. N. Kutty and N. Raghu, "Varistors Based on Polycrystalline ZnO:Cu," *Appl. Phys. Lett.*, 54 1796–1798 (1989).
15. J. Wu, C. S. Xie, K. J. Huang, A. H. Wang, and W. Y. Wang, "Low Temperature Sintering of Doped ZnO–V_2O_5 Varistors," *J. Inorg. Mater.*, 19 239–243 (2004).
16. C. S. Chen, "Effect of Dopant Valence State of Mn-ions on the Microstructure and Nonlinear Properties of Microwave Sintered ZnO–V_2O_5 Varistors," *J. Mater. Sci.*, 38 1033–1038 (2003).
17. J. J. Brown and F. A. Hummel, "Reactions Between ZnO and Selected Oxides of Elements of Groups IV and V," *Trans. Br. Ceram. Soc.*, 64 419–437 (1965).
18. R. Gopal and C. Calvo, "Crystal Structure of α-$Zn_3(VO_4)_2$," *Can. J. Chem.*, 51 1004–1009 (1973).
19. J. J. Brown and F. A. Hummel, "Dilatometric and X-ray data for zinc compounds II. Phosphates and vanadates," *Trans. Br. Ceram. Soc.*, 64 427–432 (1965).
20. V. A. Makarov, A. A. Fotiev, and L. N. Serebryakova, "Phase composition and equilibrium diagram of the V_2O_5-ZnO system," *Russ. J. Inorg. Chem.*, 16 1515–1519 (1971).
21. R. Wang, A. W. Sleight, R. Platzer, and J. A. Gardner, "Nonstoichiometric Zinc Oxide and Indium-Doped Zinc Oxide: Electrical Conductivity and ^{111}In-TDPAC Studies," *J. Solid State Chem.*, 122 166–175 (1996).
22. W. D. Kingery, *Introduction to Ceramics*, John Wiley & Sons, New York, 161–190, 1960.
23. J. I. Goldstein, D. E. Newbury, P. Echlin, D. C. Joy, C. Fiori, and E. Lifshin, *Scanning Electron Microscopy and X-Ray Microanalysis*, Plenum, New York, 75–77, 1981.